

AD-A134 231

NATURAL FREQUENCIES OF A POST WITH A LIGHTNING RETURN
STROKE ATTACHED(U) DIKEWOOD INDUSTRIES INC ALBUQUERQUE
NM F C YANG ET AL. SEP 83 AFWL-TR-83-68

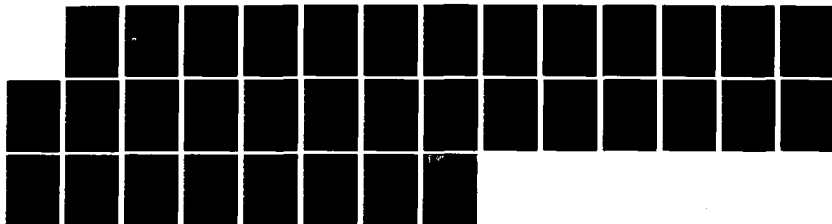
1/1

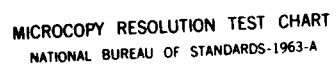
UNCLASSIFIED

F29601-82-C-0027

F/G 20/3

NL





MICROCOPY RESOLUTION TEST CHART
NATIONAL BUREAU OF STANDARDS-1963-A

AD-A134 231

NATURAL FREQUENCIES OF A POST WITH A LIGHTNING RETURN STROKE ATTACHED

F. C. Yang
K. S. H. Lee

Dikewood Corporation
1613 University Blvd
Albuquerque, NM 87102

September 1983



Final Report

Approved for public release; distribution unlimited.

DTIC FILE COPY

AIR FORCE WEAPONS LABORATORY
Air Force Systems Command
Kirtland Air Force Base, NM 87117

DTIC
ELECTE

NOV 1 1983

A

88 10 31 050

This final report was prepared by the Dikewood Corporation, Albuquerque, New Mexico, under Contract F29601-82-C-0027, Job Order 37630131 with the Air Force Weapons Laboratory, Kirtland Air Force Base, New Mexico. Lt Dennis J. Andersh (NTAA) was the Laboratory Project Officer-in-Charge.

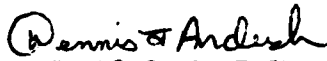
When Government drawings, specifications, or other data are used for any purpose other than in connection with a definitely Government-related procurement, the United States Government incurs no responsibility or any obligation whatsoever. The fact that the Government may have formulated or in any way supplied the said drawings, specifications, or other data, is not to be regarded by implication, or otherwise in any manner construed, as licensing the holder, or any other person or corporation; or as conveying any rights or permission to manufacture, use, or sell any patented invention that may in any way be related thereto.

This report has been authored by a contractor of the United States Government. Accordingly, the United States Government retains a nonexclusive, royalty-free license to publish or reproduce the material contained herein, or allow others to do so, for the United States Government purposes.

This report has been reviewed by the Public Affairs Office and is releasable to the National Technical Information Services (NTIS). At NTIS, it will be available to the general public, including foreign nations.

If your address has changed, if you wish to be removed from our mailing list, or if your organization no longer employs the addressee, please notify AFWL/NTAA, Kirtland AFB, NM 87117 to help us maintain a current mailing list.

This technical report has been reviewed and is approved for publication.


DENNIS J. ANDERSH
Lt, USAF
Project Officer


DAVID W. GARRISON
Lt Col, USAF
Chief, Applications Branch

FOR THE COMMANDER

ROGER S. CASE
Lt Col, USAF
Chief, Aircraft & Missile Division

DO NOT RETURN COPIES OF THIS REPORT UNLESS CONTRACTUAL OBLIGATIONS OR NOTICE ON A SPECIFIC DOCUMENT REQUIRES THAT IT BE RETURNED.

SECURITY CLASSIFICATION OF THIS PAGE (When Data Entered)

DD FORM 1473 EDITION OF 1 NOV 65 IS OBSOLETE

SECURITY CLASSIFICATION OF THIS PAGE (When Data Entered)

PREFACE

We wish to thank R. Aguero and J. Butman of Dikewood, Division of Kaman Sciences Corporation for performing the numerical calculation, and also Dr. C.E. Baum and Lt. D.J. Andersh of the Air Force Weapons Laboratory for their interest and suggestions in this effort.



Mission For	
RTIS GRA&I	<input checked="checked" type="checkbox"/>
ITIC TAB	<input type="checkbox"/>
Unannounced	<input type="checkbox"/>

A-1

CONTENTS

<u>Section</u>		<u>Page</u>
I.	INTRODUCTION	5
II.	MODELS	6
	1. RESISTIVE MODEL	6
	2. CORONA-SHEATH MODEL	6
III.	APPROACH	10
IV.	NUMERICAL RESULTS	16
V.	SUMMARY	30
	REFERENCES	31
	APPENDIX A. CHARACTERISTIC IMPEDANCE OF A LIGHTNING MODEL	33

I. INTRODUCTION

Recently, the question has been raised as to how the lightning threat to aircraft is compared to that of the high-altitude nuclear electromagnetic pulse (NEMP). The first important step towards making such a comparison possible is to characterize the electromagnetic properties of the two environments. While the high-altitude NEMP environment is quite well understood, the knowledge of the lightning environment is still in an embryonic stage. This effort is to study several possible models for characterizing the lightning return stroke and to discuss how each model can be compared with measured data.

The specific objective of this effort is to calculate the natural frequencies of a metallic post attached to a lightning channel. Two different lightning channel models will be employed for the calculation. The natural frequencies calculated can be compared with measured data when the latter become available. Such a comparison will enable one to determine the parameters inherent in the models. The electromagnetic characteristics (such as the fields) of a lightning channel can be calculated and simulated with the models.

Section II describes the two different lightning channel models. Section III details the approach which eventually leads to transcendental equations required for numerical computation. Explicit approximate analytical formulas for the natural frequencies are also derived in Section III. The transcendental equations are described by Equations 18 and 19, and the explicit analytical formulas are given by Equations 20 through 22. Section IV presents the numerical results. Section V briefly discusses the application of results to experimental measurements.

II. MODELS

In this section two lightning models, which may be referred to as (1) the resistive model and (2) the corona-sheath model, are discussed for the calculation of the natural frequencies of a post with a lightning channel attachment. The important features and the required parameters of these models are described as follows.

1. RESISTIVE MODEL

A transmission-line model has been used extensively in the past to describe the electromagnetic behavior of a lightning channel (Ref. 1). If such a model is made resistive, it would in a sense account for the presence of a corona by an introduction of a theoretical effective radius. The description of a resistive model requires the following two parameters, namely,

- the effective radius r_e , and
- the effective resistance per unit length R' .

In terms of these two parameters, the lightning channel together with a corona has a characteristic impedance $Z_c^r(s)$ given by (Ref. 2 and Appendix A)

$$Z_c^r(s) = \frac{Z_0}{2\pi} \psi^r(s) \quad (1)$$

where

$$\psi^r(s) = \left\{ \left[\ln(sr_e/c) \right]^2 - \frac{2\pi R' \ln(sr_e/c)}{s\mu_0} \right\}^{1/2}$$

$s = j\omega$ is the complex frequency, Z_0 , c , μ_0 are, respectively, the free-space wave impedance, speed of light, permeability, and the superscript r is used to indicate resistive model quantities.

2. CORONA-SHEATH MODEL

The corona-sheath model has been suggested in Reference 3 for a lightning channel and its surrounding corona. In this model, the lightning current

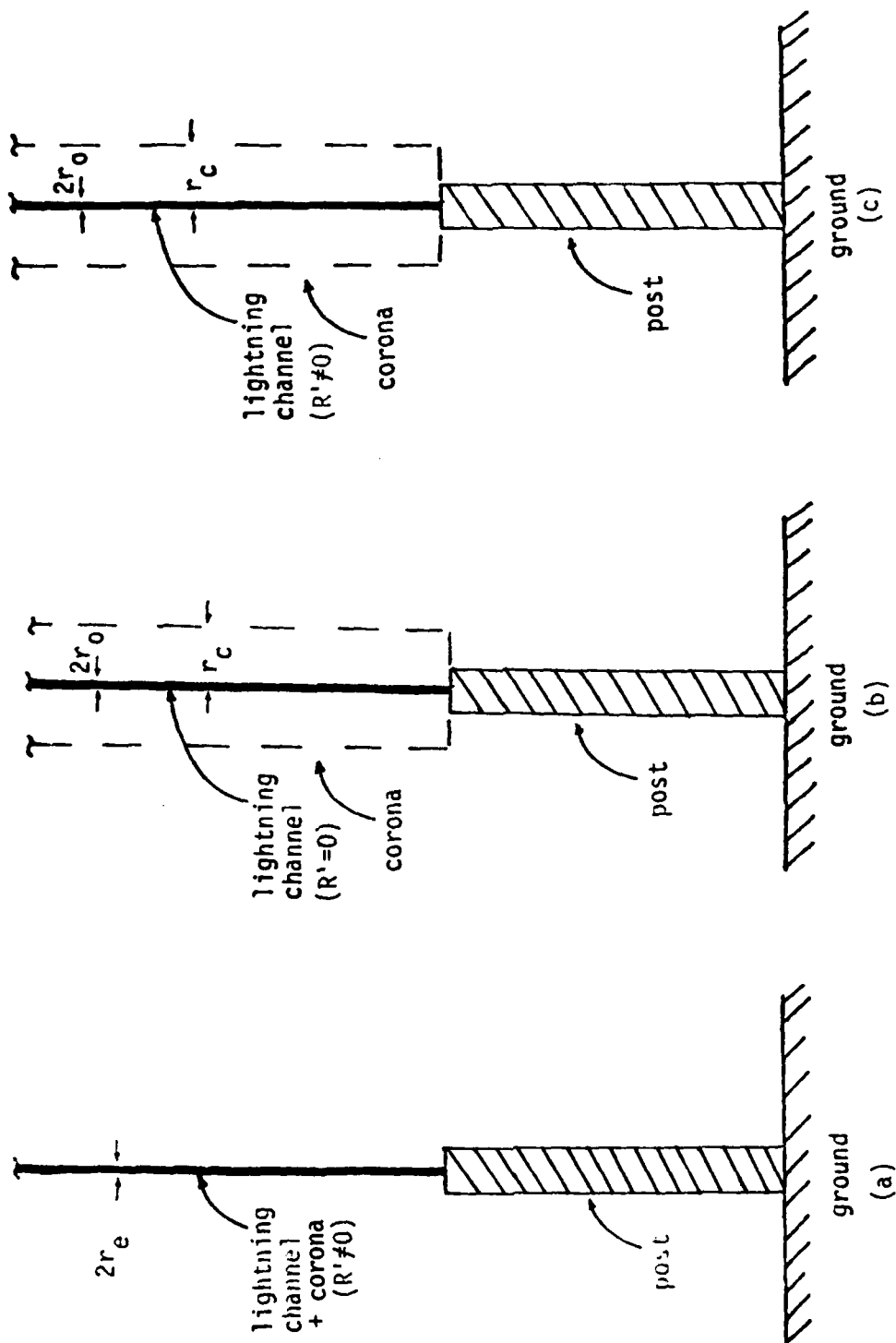


Figure 1. Various models for lightning which strikes a metallic post. (a) Resistive model, (b) corona-sheath model, and, (c) a general representation for both (a) and (b). In the figure, R' is the resistance per unit length.

flows only in the perfectly conducting center channel, while all the electric charges reside on an effective corona surface. This model is shown in Figure 1b together with a post. The required parameters for the corona-sheath model are

- the effective radius of the lightning center channel r_0 , and
- the effective radius of the corona surface r_c .

The effective corona radius r_c is related to the charge per unit length of the corona Q' via

$$r_c = \frac{|Q'|}{2\pi\epsilon_0 E_b}, \quad E_b \approx 3 \times 10^6 \text{ V/m} \quad (2)$$

where E_b and ϵ_0 are the air breakdown electric field and the permittivity of the surrounding air. This model can also be considered as a transmission line with the characteristic impedance (Appendix A)

$$Z_c^c(s) = \frac{Z_0}{2\pi} \psi^c(s) \quad (3)$$

where

$$\psi^c(s) \approx \left\{ \ln\left(\frac{sr_0}{c}\right) \ln\left(\frac{sr_c}{c}\right) \right\}^{1/2}$$

and the superscript c is used to indicate corona-sheath model quantities. Clearly, the above two lightning models are special cases of a more complicated model depicted in Figure 1c, which allows for resistivity in the center channel and, therefore, has the following corresponding characteristic impedance (Appendix A)

$$\begin{aligned} Z_c(s) &= \frac{Z_0}{2\pi} \psi(s) \\ &\approx \frac{Z_0}{2\pi} \left\{ \ln\left(\frac{sr_0}{c}\right) \ln\left(\frac{sr_c}{c}\right) - \frac{2\pi R' \ln sr_c/c}{s\mu_0} \right\}^{1/2} \end{aligned} \quad (4)$$

Section III describes an approach to solving this more general model. The two special models given by Equations 1 and 3 can then be obtained from Equation 4 by taking

- $r_o = r_c = r_e$ for the resistive model, and
- $R' = 0$ for the corona-sheath model.

III. APPROACH

The original problem of Figure 1c where the post sits vertically on a perfectly conducting ground is equivalent to that of Figure 2 where the images are used to account for the ground effects. The natural modes of the imaged problem can be obtained by solving for the nontrivial solutions of the following homogeneous integro-differential equation with certain appropriate boundary conditions (Ref. 4 and the references quoted therein):

$$\left(\frac{d^2}{dz^2} - \frac{s^2}{c^2}\right) \int_{-\ell}^{\ell} \frac{e^{-(s/c) \sqrt{a^2 + (z - z')^2}}}{4\pi \sqrt{a^2 + (z - z')^2}} I(z') dz' = 0, \quad |z| \leq \ell \quad (5)$$

where a and ℓ are, respectively, the radius and length of the post.

Equation 5 can first be reduced to an integral equation

$$\int_{-\ell}^{\ell} \frac{e^{-(s/c) \sqrt{a^2 + (z - z')^2}}}{\sqrt{a^2 + (z - z')^2}} I(z') dz' = B \cosh(sz/c), \quad |z| \leq \ell \quad (6)$$

where B is the integration constant and the following symmetry condition has been imposed

$$I(z) = I(-z) \quad (7)$$

Additional conditions are required for solving Equation 6: they are the continuation of current and the equality of potential at the attachment point of the post and lightning channel, i.e., at $z = \ell$,

$$\begin{aligned} I_-(\ell) &= I_+(\ell) = I(\ell) \\ \phi_-(\ell) &= \phi_+(\ell) = \phi(\ell) \end{aligned} \quad (8)$$

where the subscript - or + indicates quantities at the post side or the lightning side.

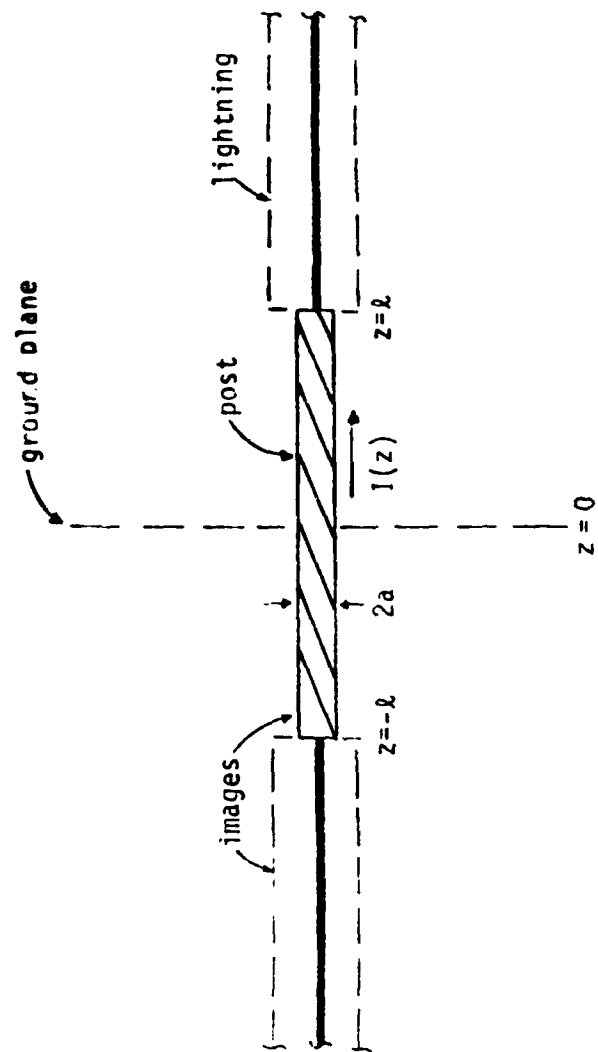


Figure 2. An equivalent representation of Figure 1c, with the ground effect being accounted for with images.

Since the potential at the post side is given by

$$\phi_- = -\frac{1}{4\pi s \epsilon_0} \frac{d}{dz} \left[\frac{e^{-(s/c) \sqrt{a^2 + (z - z')^2}}}{\sqrt{a^2 + (z - z')^2}} I(z') dz' \right] \Big|_{z = \ell} \quad (9)$$

and the potential at the lightning side is equal to the potential drop for a current I_+ flowing through $Z_C(s)$, i.e.,

$$\phi_+ = I_+ Z_C(s) \quad (10)$$

Equation 8 is then equivalent to

$$\frac{d}{dz} \left[\frac{e^{-(s/c) \sqrt{a^2 + (z - z')^2}}}{\sqrt{a^2 + (z - z')^2}} I(z') dz' \right] \Big|_{z = \ell} = -4\pi s \epsilon_0 Z_C(s) I(\ell) \quad (11)$$

which can be combined with Equation 6 to solve for B and give

$$\left[\frac{e^{-(s/c) \sqrt{a^2 + (z - z')^2}}}{\sqrt{a^2 + (z - z')^2}} I(z') dz' \right]_{-\ell}^{\ell} = \frac{-2\psi(s) I(\ell)}{\sinh(s\ell/c)} \cosh(sz/c) \quad (12)$$

This is the final integral equation that is needed to solve for the natural modes of the problem posed in Figure 2.

Since the radius a of the post is much smaller than its length ℓ , an asymptotic theory can be used to solve Equation 12. First, rewrite Equation 12 in the following form

$$I(z) \int_{-\ell}^{\ell} \frac{1}{\sqrt{a^2 + (z - z')^2}} dz' + \int_{-\ell}^{\ell} \frac{I(z') e^{-(s/c) \sqrt{a^2 + (z - z')^2}} - I(z)}{\sqrt{a^2 + (z - z')^2}} dz' \\ = - \frac{2\psi(s)I(\ell)}{\sinh(s\ell/c)} \cosh(sz/c) \quad (13)$$

or equivalently,

$$I(z)\Omega(z) + \frac{2\psi(s)I(\ell)}{\sinh(s\ell/c)} \cosh(sz/c) \\ = - \int_{-\ell}^{\ell} \frac{I(z') e^{-(s/c) \sqrt{a^2 + (z - z')^2}} - I(z)}{\sqrt{a^2 + (z - z')^2}} dz' \quad (14)$$

where

$$\Omega(z) = \sinh^{-1}\left(\frac{\ell + z}{a}\right) + \sinh^{-1}\left(\frac{\ell - z}{a}\right) \quad (15)$$

and is a slowly varying function of z with $\Omega(0) = 2 \sinh^{-1}(\ell/a) \approx 2 \ln(2\ell/a)$. Using the fact that $\Omega(z) \approx \Omega(0) \gg 1$ and $|\psi(s)| \gg 1$, one can expand s and $I(z)$ in the following fashion

$$s = s^{(0)} + s^{(1)} + \dots \\ I = I^{(0)} + I^{(1)} + \dots \quad (16)$$

where $s^{(m)}$, $I^{(m)}$ are of the order of $1/\Omega^m$ or $1/\psi^m$. Substituting Equation 16 in Equation 14, one has

$$I^{(0)}(z) = A_0 \frac{\Omega(0)}{\Omega(z)} \cosh(s^{(0)} z/c) \quad (17)$$

$$1 + \frac{2\psi(s^{(0)})}{\Omega(\ell)} \coth(s^{(0)} \ell/c) = 0 \quad (18)$$

and

$$2 \frac{s^{(1)} \ell}{c} = \left\{ \Omega(0) + \frac{2\Omega(0)}{\Omega(\ell)} \frac{c}{\ell} \cosh^2 \left(\frac{s^{(0)} \ell}{c} \right) \frac{d\psi(s^{(0)})}{ds^{(0)}} \right\}^{-1} \\ \cdot e^{s^{(0)} \ell / c} \sinh \left(\frac{s^{(0)} \ell}{c} \right) E \left(\frac{4s^{(0)} \ell}{c} \right) \quad (19)$$

where (Ref. 5)

$$E(\zeta) \equiv E_1(\zeta) + \ln \zeta + \gamma$$

$$E_1(\zeta) \equiv \int_{\zeta}^{\infty} \frac{e^{-t}}{t} dt \equiv \text{exponential integral}$$

$$\gamma \equiv 0.577\dots \equiv \text{Euler's constant}$$

When $|\psi(s)| \rightarrow \infty$, Equations 16 through 19 agree, as they should, with Equations 16 and 17 of Reference 4 where a post without a lightning attachment was discussed. Equation 18 can be used to solve for $s^{(0)}$, from which $s^{(1)}$ can then be calculated via Equation 19.

When $R' \ell \gg Z_0$ and/or $a \gg (r_0, r_c, r_e)$, one has $|\psi(s)| \gg \Omega(\ell)$, and Equation 18 can be approximately solved. The approximate solution is

$$\frac{s_n^{(0)} \ell}{c} \simeq j \frac{(2n+1)\pi}{2} - \frac{\Omega(\ell)}{2\psi_n}, \quad n = 0, 1, 2, \dots \quad (20)$$

where $\psi_n = \psi(s)$ with $s = j(2n+1)\pi c/(2\ell)$, i.e.,

$$\psi_n \simeq \left\{ \left(\ln \left[\frac{2\ell}{(2n+1)\pi r_0} \right] - j\frac{\pi}{2} \right) \left(\ln \left[\frac{2\ell}{(2n+1)r_c \pi} \right] - j\frac{\pi}{2} \right) \right. \\ \left. - \frac{R' \ell}{Z_0} \frac{4j}{(2n+1)} \left(\ln \left[\frac{2\ell}{(2n+1)r_c \pi} \right] - j\frac{\pi}{2} \right) \right\}^{1/2} \quad (21)$$

Furthermore, Equation 19 can be approximated by

$$\frac{s_n^{(1)} \lambda}{c} \approx - \frac{1}{2\Omega(0)} \left\{ \ln[(2n+1)2\pi] + \gamma + j \left[\frac{\pi}{2} - \frac{1}{(2n+1)2\pi} \right] \right\} \quad (22)$$

In Equations 20 through 22, $\Omega(\lambda) \approx \ln(4\lambda/a)$, $\Omega(0) \approx 2\ln(2\lambda/a)$, and the subscript n indicates the quantity referring to the n -th natural mode.

The sum, $s_n^{(0)} + s_n^{(1)}$, obtained from Equations 20 through 22 gives the approximate analytical formula for the natural frequencies of a post with a lightning channel attachment. The accuracy of the approximate analytical formula will be checked against the numerical results computed from Equations 18 and 19 in Section IV. It is seen from Equation 20 and 22 that the effect of a channel attachment on the post's natural frequencies is entirely accounted for by the last term of Equation 20. This term is proportional to $(R'\lambda/Z_0)^{-1/2}$ when the lightning channel is highly resistive, and vanishes, as expected, when $R' \rightarrow \infty$.

IV. NUMERICAL RESULTS

Equations 18 and 19 were numerically solved on a microcomputer for $\psi(s)$ given by Equation 4. The results of $s^{(0)} + s^{(1)}$ are given in Figures 3 through 14 for post radius $a = 0.05$ m, and various post length λ and lightning parameter values. The lightning parameters are the corona radius r_c , the channel radius r_0 , the combined effective radius r_e , and the effective resistance R' per unit length (Fig. 1).

Figures 3 through 9 are the natural-frequency plots for the resistive model with $r_0 = r_c = r_e$ and nonzero $R'\lambda/Z_0$. Figures 3 and 4 show the effect of the channel resistance R' on the post's natural frequencies for two different values of effective lightning radius r_e . The imaginary part of the natural frequencies remains almost unchanged as $R'\lambda/Z_0$ varies. On the other hand, the absolute value of the real part (i.e., the decaying constant) increases when $R'\lambda/Z_0$ decreases. This is expected because a post with a lightning attachment of lower resistance is different from a post without a lightning attachment.

Figures 5 and 6 show the effect of the effective lightning radius r_e on the post's natural frequencies for $R'\lambda/Z_0 \geq 10^4$ and equal to 10. The natural frequencies are found to depend only weakly on r_e . This is because the dependence of the characteristic impedance Z_c of a lightning channel on r_e is logarithmic. Also, when the channel is very resistive, i.e., when $R'\lambda/Z_0 \geq 10^4$, the natural frequencies become independent of r_e , and are the same as those of a post without a lightning attachment.

Figures 7 through 9 show the effect of the post length λ on the natural frequencies. When $R'\lambda/Z_0$ is large (i.e., $\geq 10^4$), the decaying constant increases as λ decreases. The reason is that there is more radiation loss for a thicker post of a given length. When $R'\lambda/Z_0$ is small (≤ 10), the dependence of the normalized natural frequency on λ is weak. This is attributable to the fact that the damping of the post current is mainly caused by the leakage into the lightning channel whose dependence on λ is logarithmic.

Figures 10 through 14 give the natural frequencies of the corona-sheath model with $R'\lambda/Z_0 \approx 0$. Figures 10 and 11 show the effect of the corona radius r_c whereas Figures 12 through 14 show the effect of the post length λ on the

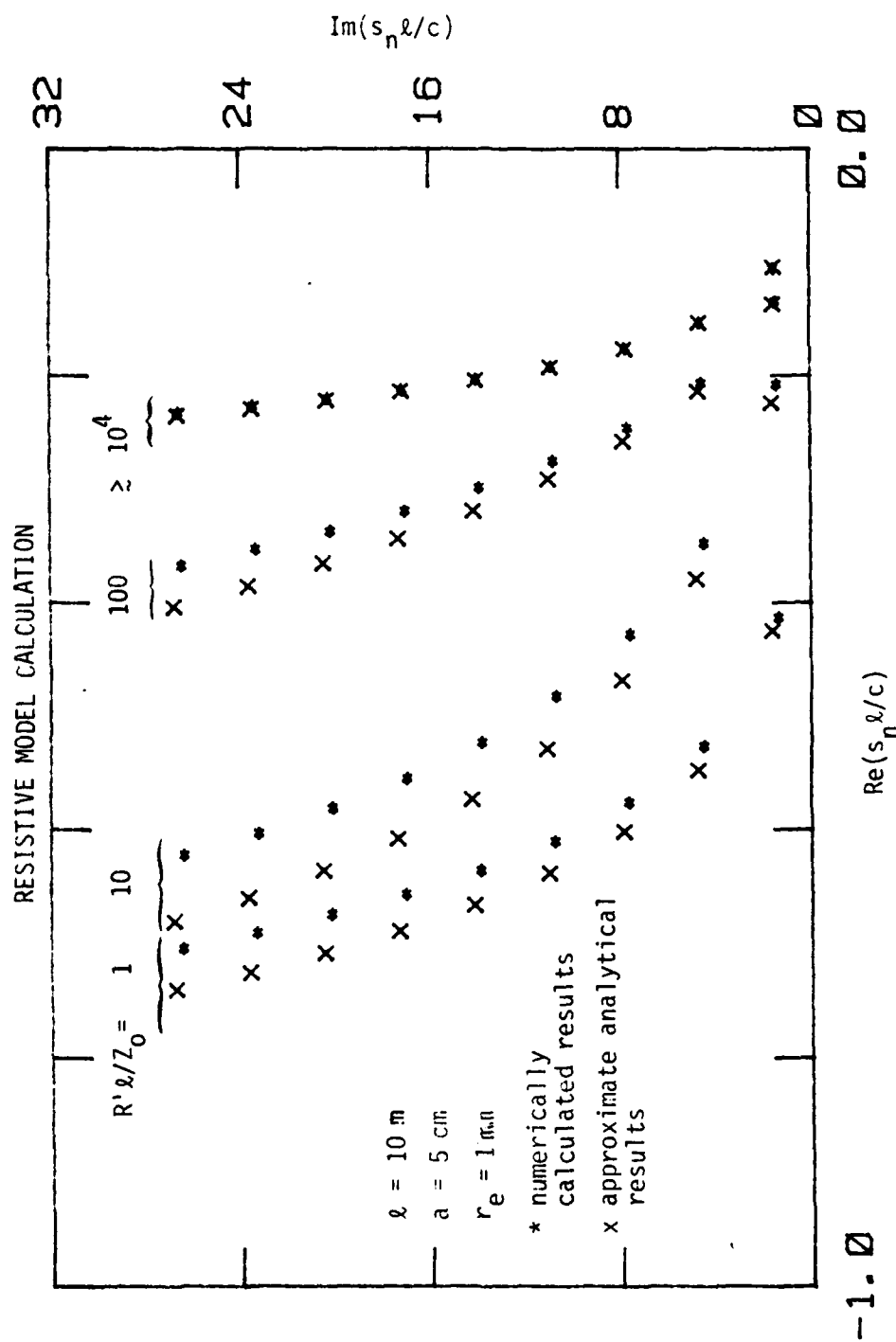


Figure 3. Normalized natural frequencies of a post of 10 m long, 5 cm in radius with a lightning attachment of $r_e = 1 \text{ m}$ and various $R'l$. The branch of poles with $R'l/Z_0 \geq 10^4$ also corresponds to the poles of a post in free space.

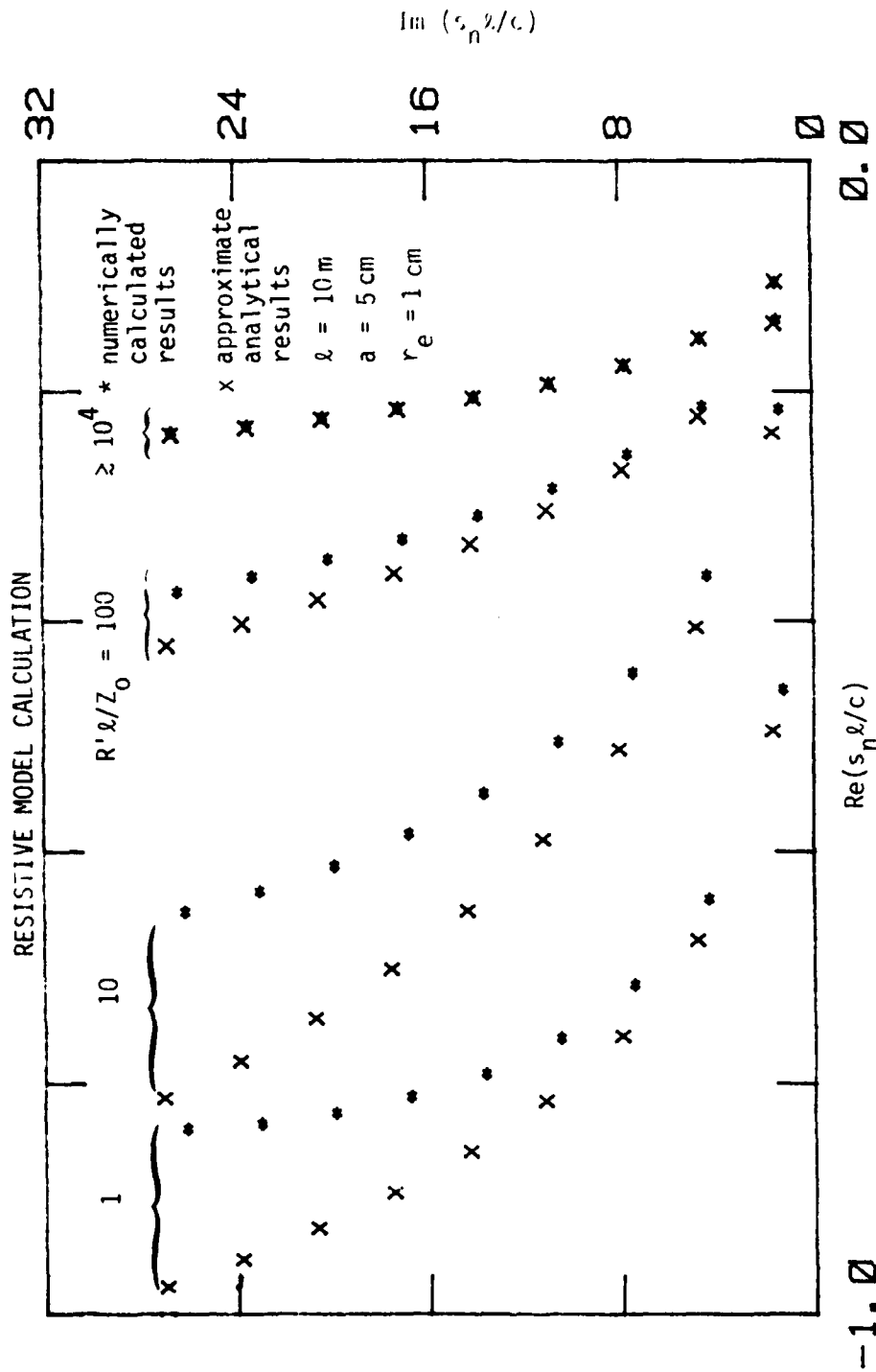


Figure 4. Normalized natural frequencies of a post of 10 m long, 5 cm in radius, with a lightning attachment of $r_a = 1 \text{ cm}$ and various R' . The branch of poles with $R' l/Z_0 \geq 10^4$ also corresponds to the poles of a post in free space.

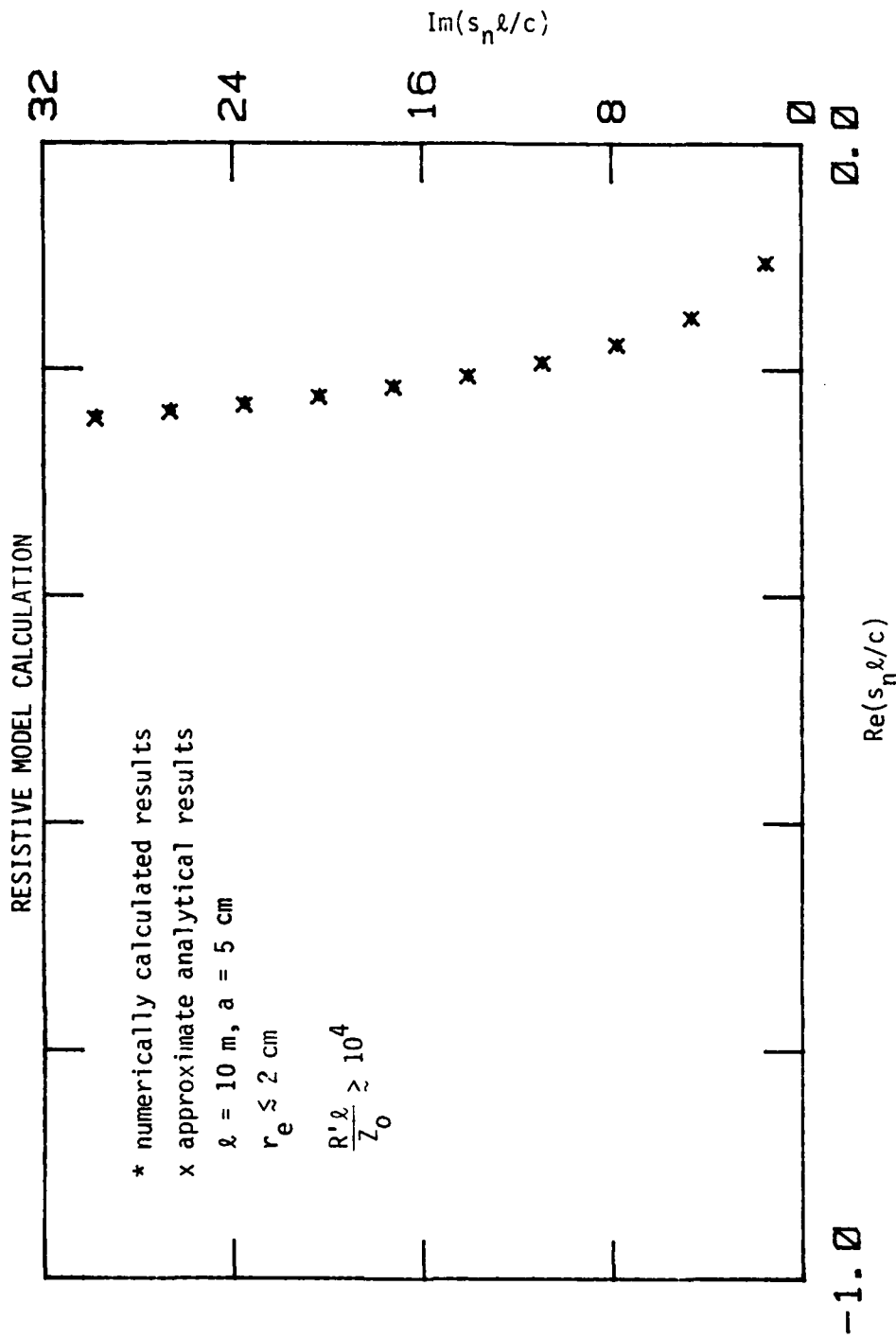


Figure 5. Normalized natural frequencies of a post of 10 m long, 5 cm in radius, with a lightning attachment of $r_e \leq 2 \text{ cm}$ and $R'l/Z_0 \geq 10^4$. These poles also correspond to those of a post in free space.

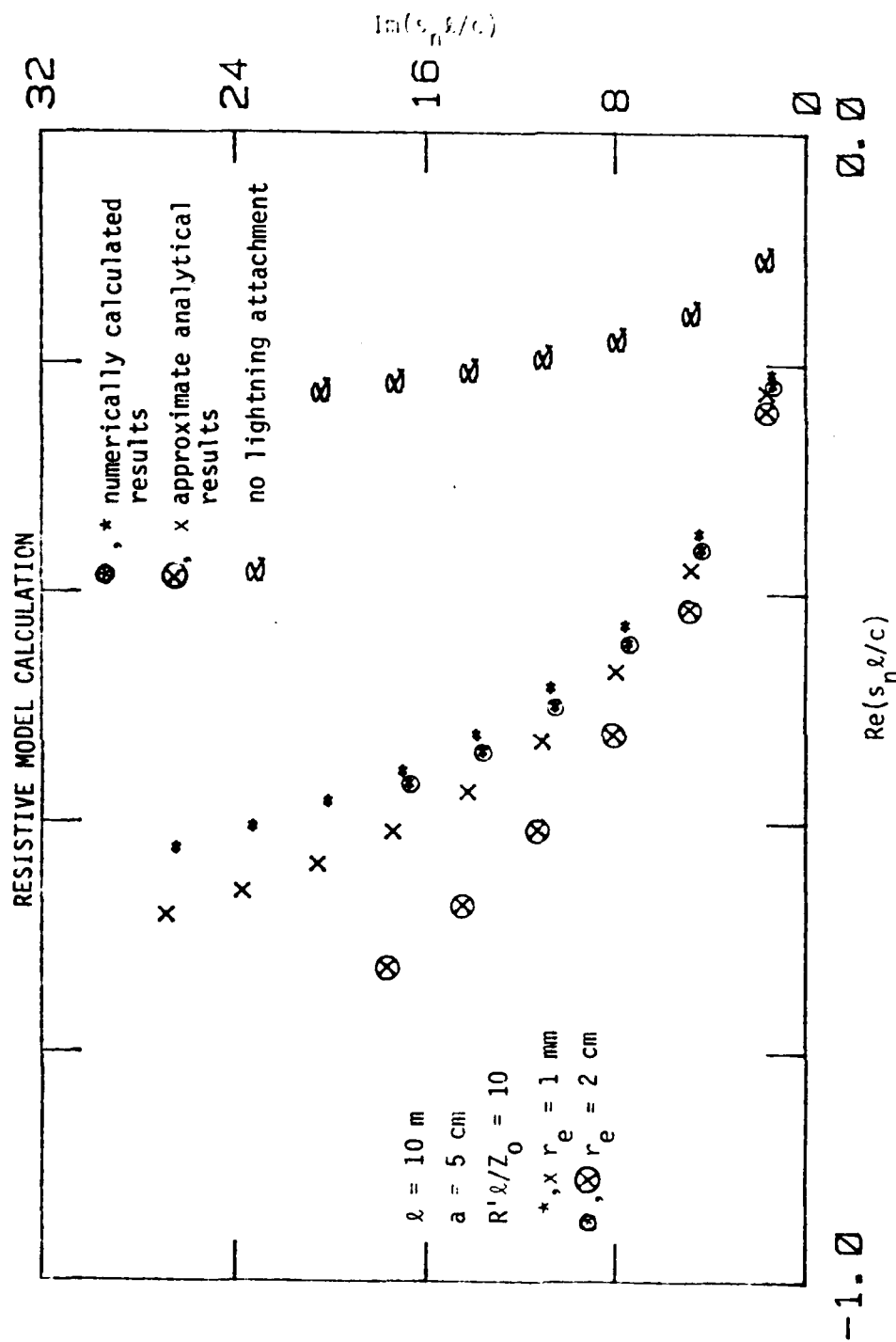


Figure 6. Normalized natural frequencies of a post of 10 m long, 5 cm in radius, with a lightning attachment of $R'l/Z_0 = 10$ and various r_e . In the figure, the natural frequencies for a post with no lightning attachment are also included.

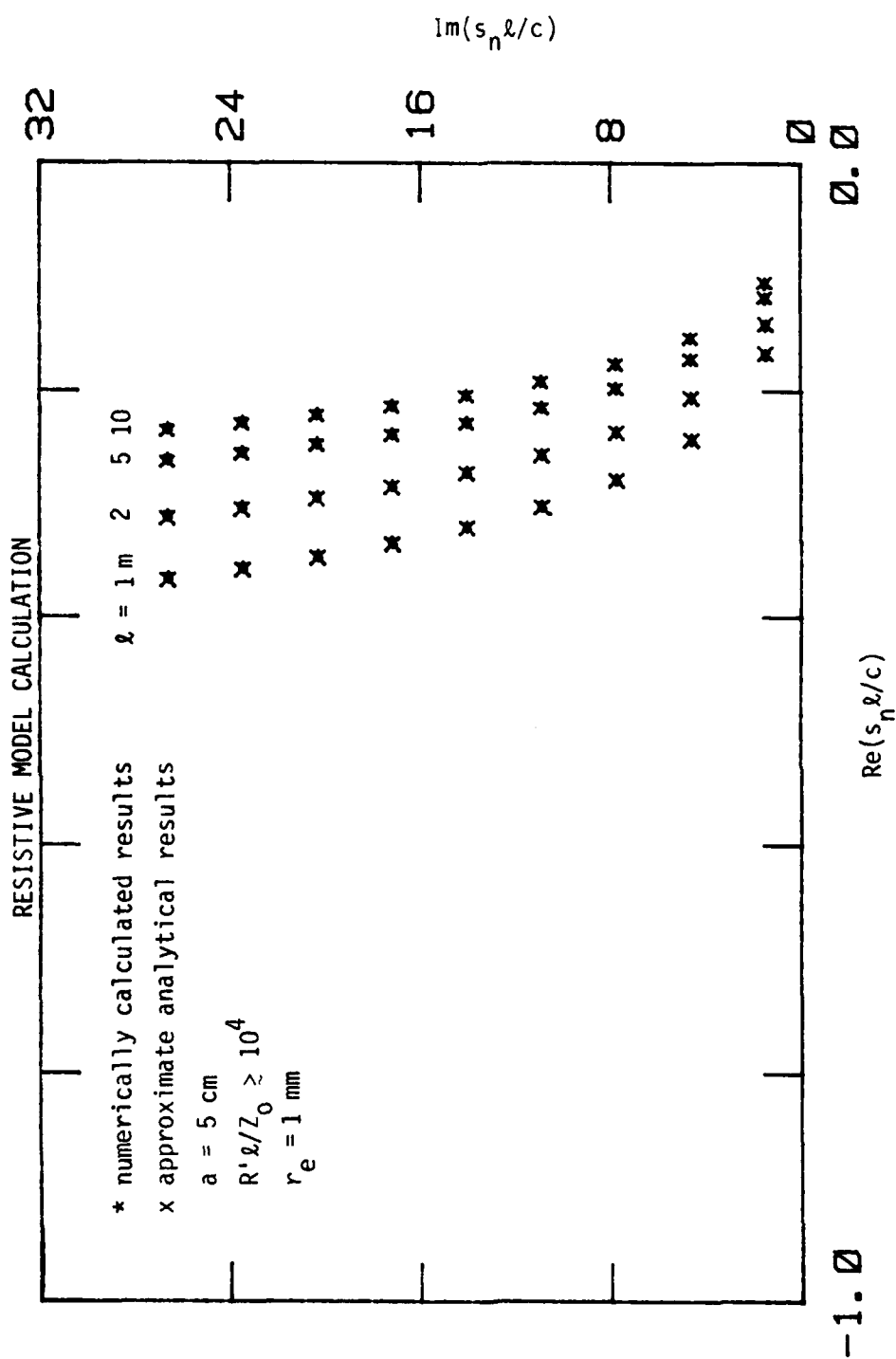


Figure 7. Normalized natural frequencies of a post of various length and 5 cm in radius, with a lightning attachment of $r = 1 \text{ mm}$ and $R'l/Z_0 \geq 10^4$. These poles also correspond to those of a post in free space.

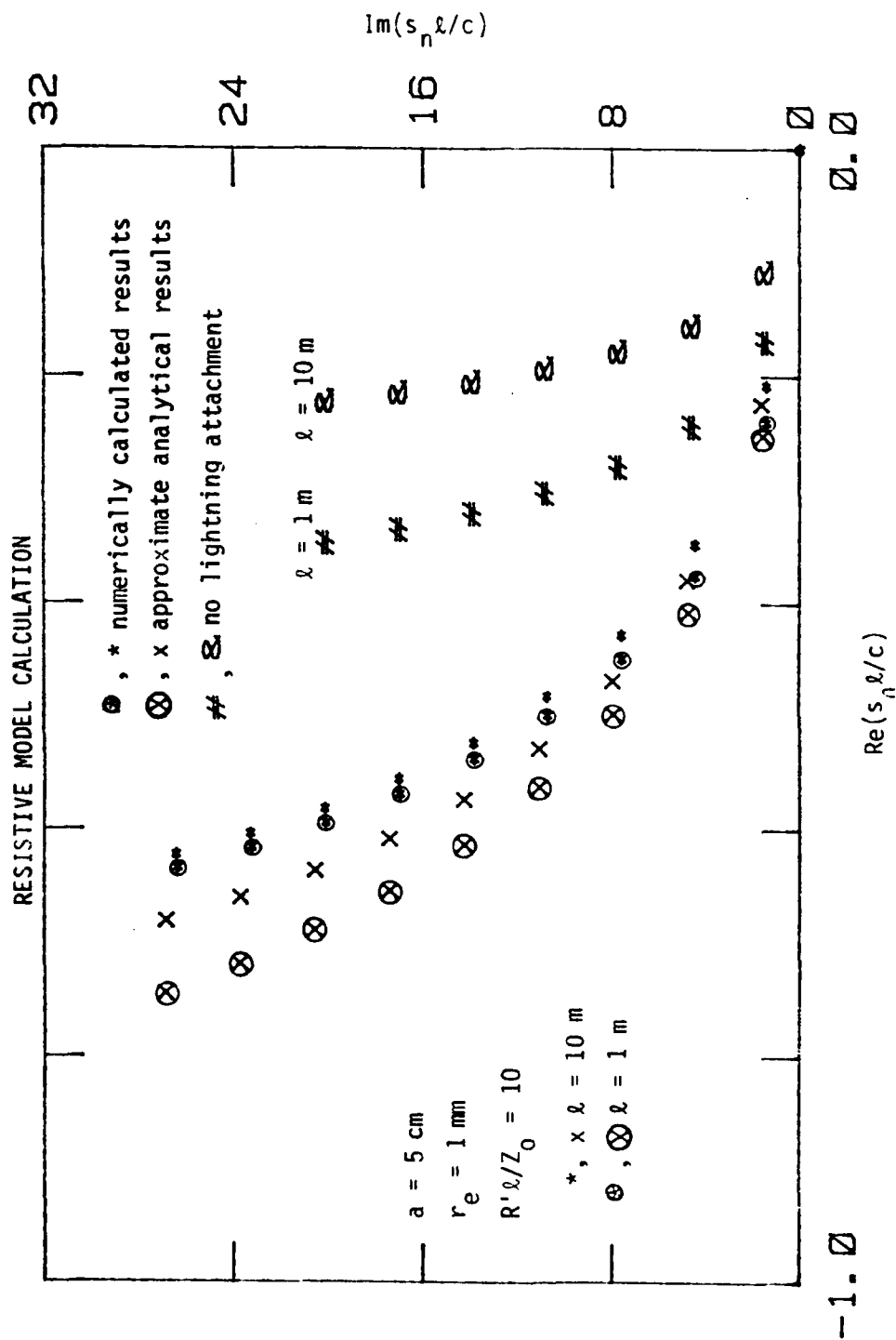


Figure 8. Normalized natural frequencies of a post of various length and 5 cm in radius, with a lightning attachment of $r_e = 1 \text{ mm}$ and $R'l/Z_0 = 10$. In the figure, the natural frequencies for posts with no lightning attachment are also included.

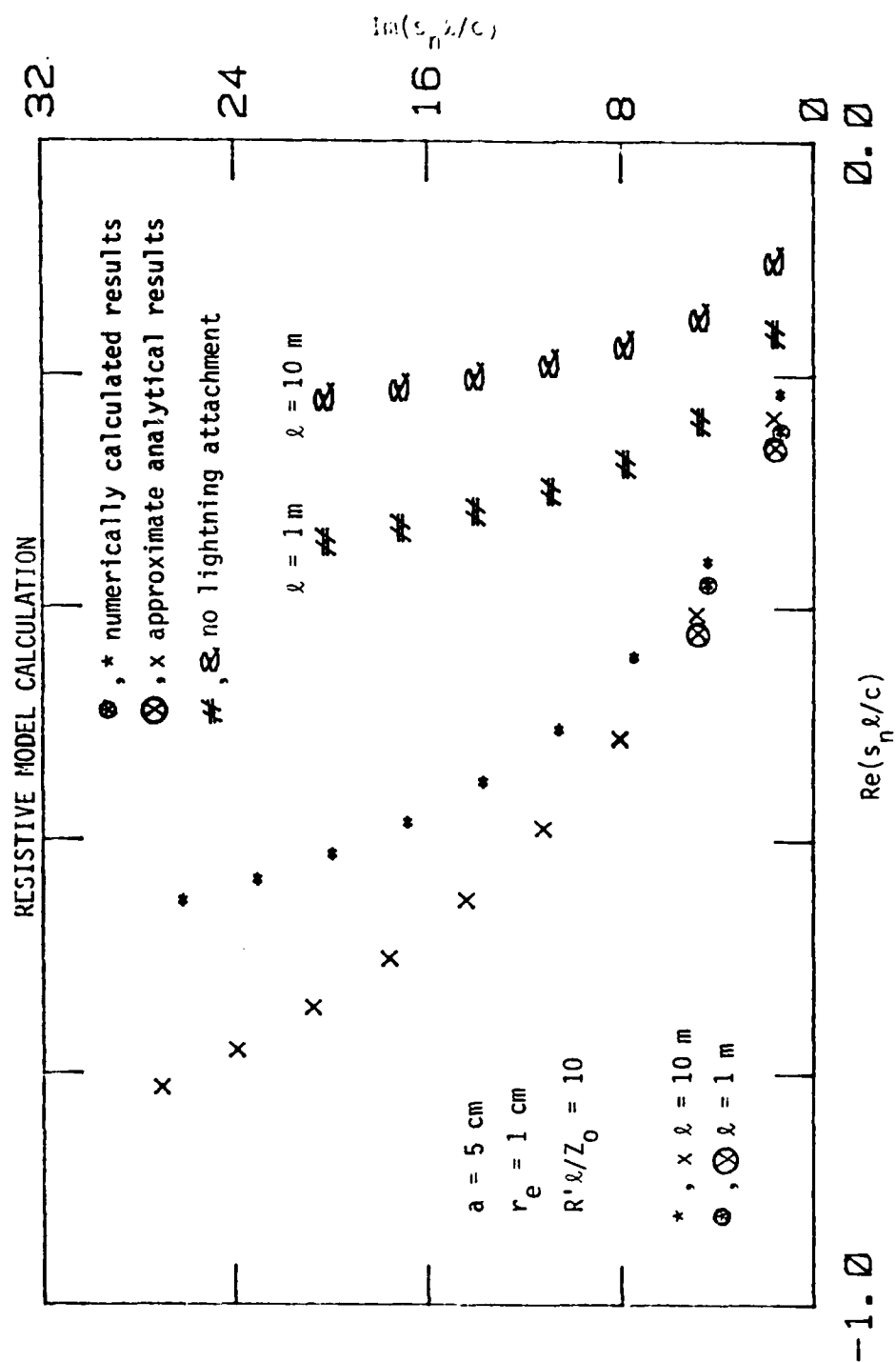


Figure 9. Normalized natural frequencies of a post of various length and 5 cm in radius, with a lightning attachment of $r_e = 1 \text{ cm}$ and $R'l/Z_0 = 10$. In the figure, the natural frequencies for posts with no lightning attachment are also included.

CORONA SHEATH & RESISTIVE MODEL CALCULATION

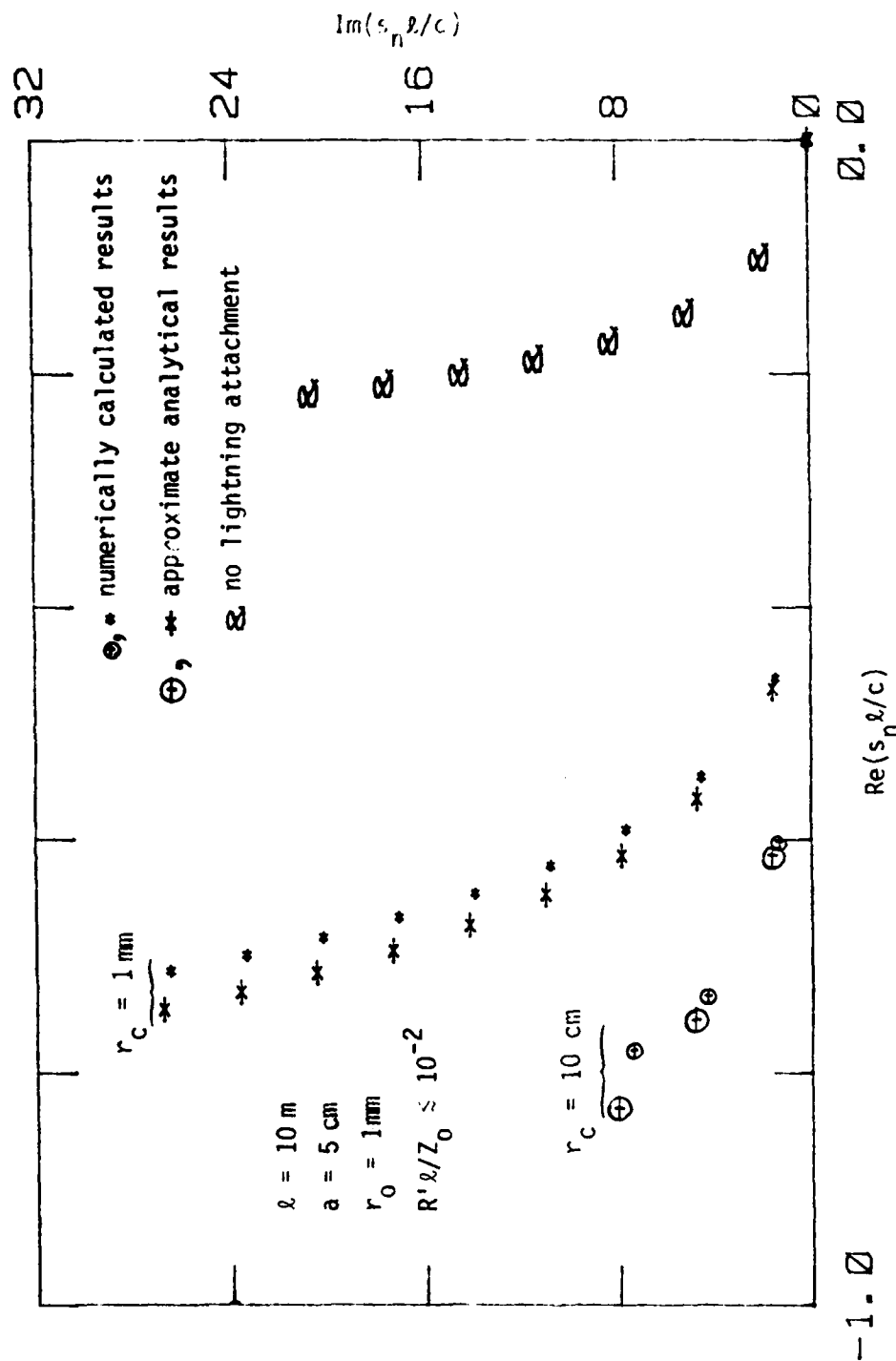


Figure 10. Normalized natural frequencies of a post of 10m long and 5 cm in radius with a lightning attachment of $R'\lambda/Z_0 \approx 10^{-2}$, $r_0 = 1 \text{ mm}$ and various r_c . In the figure, the natural frequencies for a post with no lightning attachment are also included.

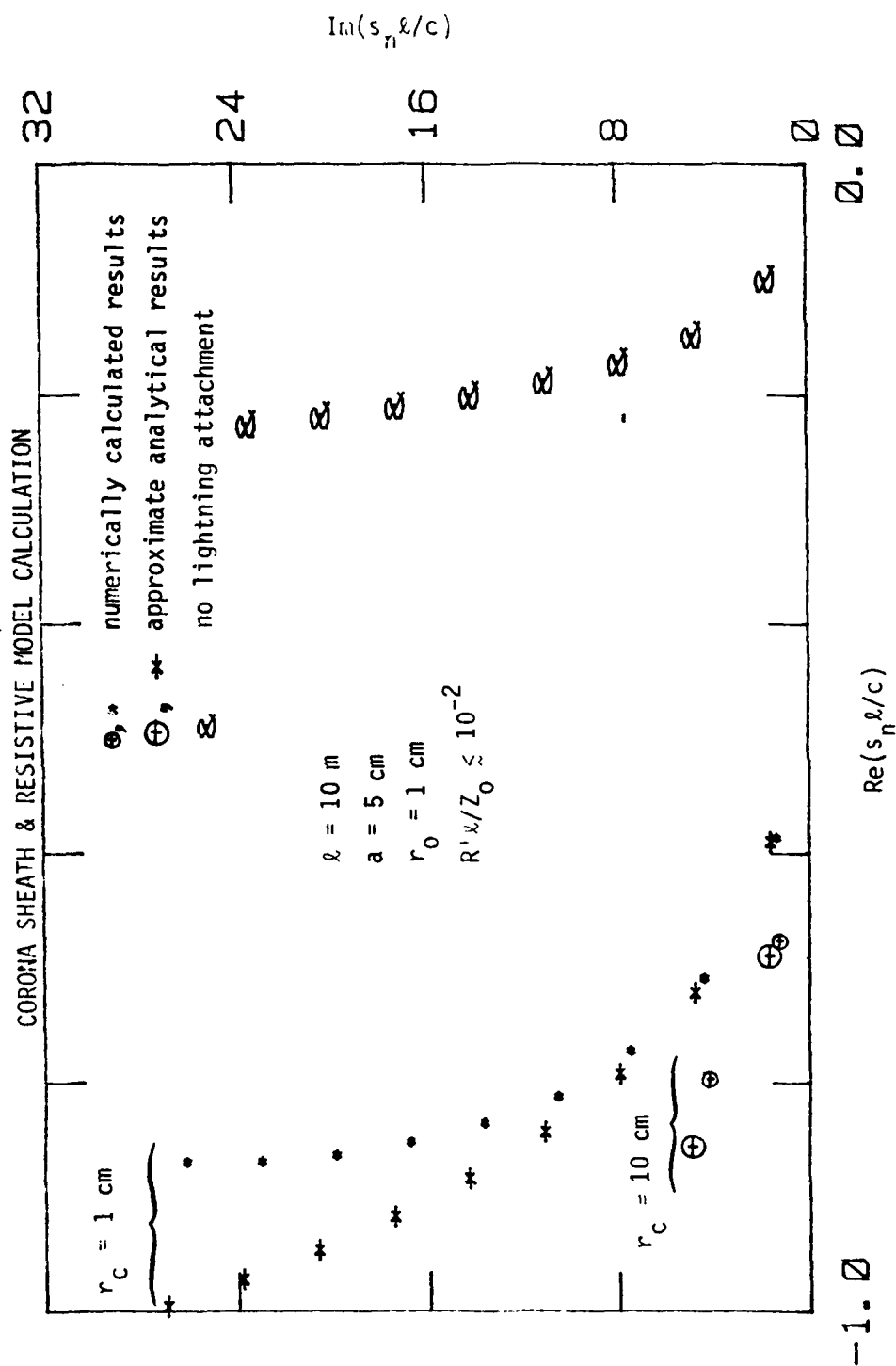


Figure 11. Normalized natural frequencies of a post of 10 m long and 5 cm in radius, with a lightning attachment of small $R' l / Z_0$, $r_0 = 1 \text{ cm}$ and various r_c . In the figure, the natural frequencies for a post with no lightning attachment are also included.

CORONA SHEATH & RESISTIVE MODEL CALCULATION

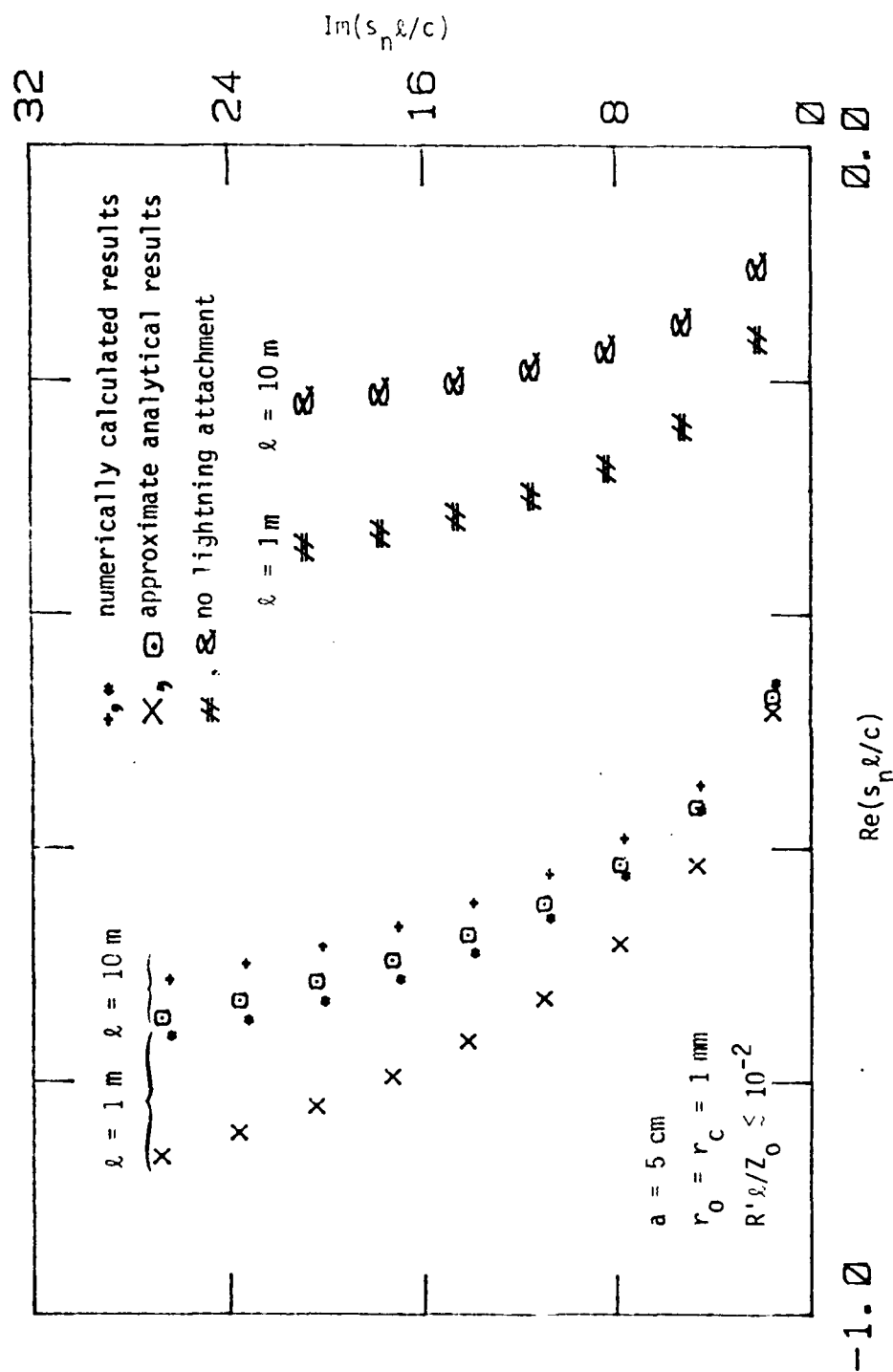


Figure 12. Normalized natural frequencies of a post of various length and 5 cm in radius with a lightning attachment of small $R' l / Z_0$ and $r_0 = r_c = 1 \text{ mm}$. In the figure, the natural frequencies for posts with no lightning attachment are also included.

CORONA SHEATH MODEL CALCULATION

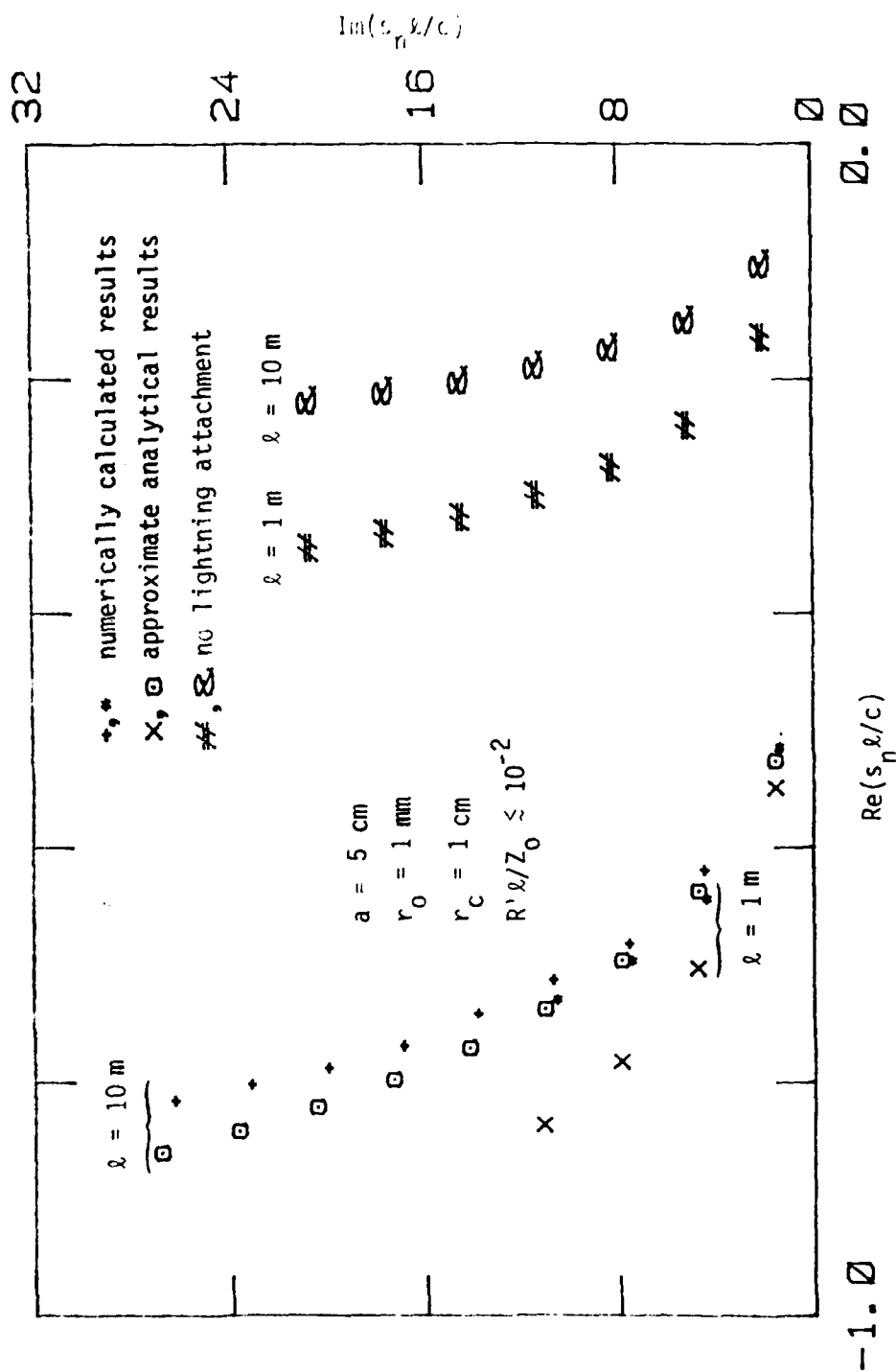


Figure 13. Normalized natural frequencies of a post of various length and 5 cm in radius, with a lightning attachment of small $R'l/Z_0$, $r_0 = 1 \text{ mm}$, and $r_c = 1 \text{ cm}$. In the figure, the natural frequencies for posts with no lightning attachment are also included.

CORONA SHEATH & RESISTIVE MODEL CALCULATION

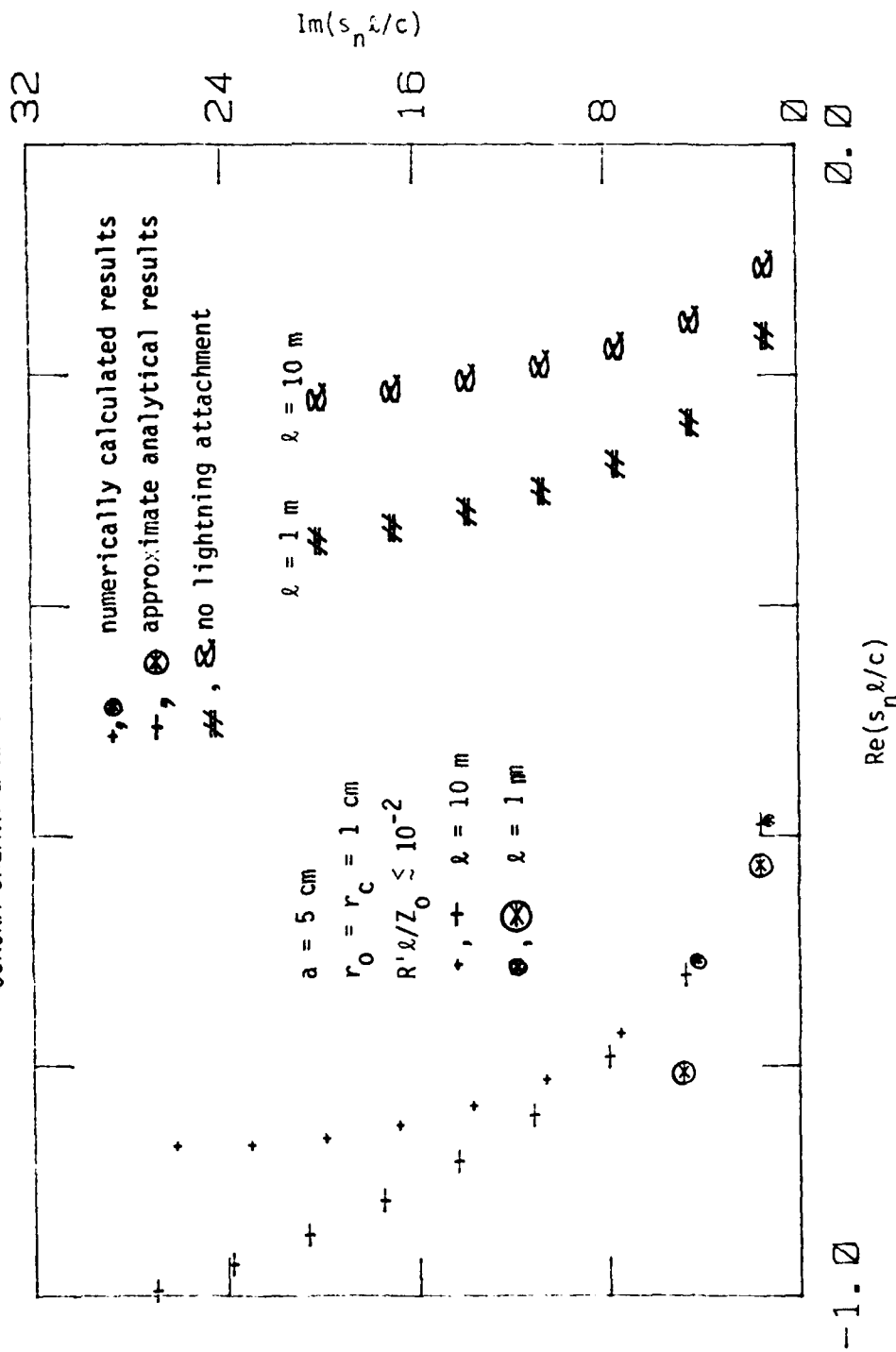


Figure 14. Normalized natural frequencies of a post of various length and 5 cm in radius, with a lightning attachment of small $R'l/Z_0$ and $r_0 = r_c = 1 \text{ cm}$. In the figure, the natural frequencies for posts with no lightning attachment are also included.

post's natural frequencies. The normalized natural frequencies are nearly independent of λ .

The approximate analytical results given by Equations 20 and 22 are also plotted in Figures 3 through 14 for comparison with the numerical results. The agreement is generally excellent for the lower-order modes.

V. SUMMARY

In summary, this report gives the calculation of the natural frequencies of a metallic post on a ground plane with a lightning channel attached and with various post radii and post lengths.

As measured frequency data become available, they can be compared to the model calculation presented in this report. Such a comparison will enable one to determine the model parameters, such as the effective resistance per unit length R' , the effective radius of the lightning center channel r_0 , and the effective radius of the corona surface r_c .

A closer observation of all the figures presented in Section IV indicates that there is a definite relationship between the natural frequencies ($s_n \ell/c$) and R' , r_0 , r_c . In particular, the natural frequencies move away from the $j\omega$ -axis when R' becomes greater. This trend enables one to quickly determine the rough ranges of the model parameters R' , r_0 , r_c for a lightning attached to a post when one compares the poles extracted from the measured post current with these calculated poles. For example, if the post length $\ell = 10$ m, and the post radius $a = 5$ cm, and if the measured data satisfy the inequality $|\operatorname{Re}(s_n \ell/c)| < 0.4$, one could quickly obtain the conditions from the trend that $r = r_c < 0.2$ cm and $R' \ell/Z_0 \geq 100$, whereas the more exact values for r_0 , r_c , and R' have to be determined by a comparison of measured poles with the calculated poles such as those in Figure 3. On the other hand, if the measured data show $|\operatorname{Re}(s_n \ell/c)| > 0.4$, the condition that $R' \ell/Z_0 \leq 1$ would be obtained, while the more exact values for r_0 , r_c and R' have to be determined by comparing the measured poles with the calculated curves such as those of Figures 3, 4, 10 and 11.

From the obtained model parameters R' , r_0 , r_c and the measured post current, one can synthesize the lightning current distribution, from which other electromagnetic characteristics such as the fields generated can be calculated.

The model employed in this report involves the assumption that the ground is perfectly conducting and infinite in extent. This assumption is not expected to introduce significant error, since the fields are quite localized along the lightning channel and the measuring post.

REFERENCES

1. Volland, H., "A Wave Guide Model of Lightning Currents and Their Electromagnetic Field," on Lightning Technology, NASA Conference Publication 2/28, FAA-RD-80-30, pp. 3-19, April 1980.
2. King, R.W.P., et al., Antennas in Matter, the MIT Press, Cambridge, Massachusetts, 1981.
3. Baum, C.E., "Properties of Lightning Leader Pulses," Lightning Phenomenology Notes, Note 2, Air Force Weapons Laboratory, Kirtland AFB, New Mexico, December 1981.
4. Marin, L., "Natural Modes of Certain Thin-Wire Structures," Interaction Notes, Note 186, Air Force Weapons Laboratory, Kirtland AFB, New Mexico, August 1974.
5. Abramowitz, M., and I.N. Stegun, Editors, Handbook of Mathematical Functions, National Bureau of Standards, AMS-55, 1964.

APPENDIX A

CHARACTERISTIC IMPEDANCE OF A LIGHTNING MODEL

In this appendix, the characteristic impedance for the lightning model depicted in Figure 1c will be derived. This impedance is reducible to the two simpler cases corresponding to the lightning models of Figures 1a and 1b.

In Reference 2, it is shown that a perfectly conducting wire of radius r has a characteristic impedance Z_C^0 given by

$$Z_C^0 \approx \frac{Z_0}{2\pi} K_0(sr/c) \quad (A.1)$$

Since the inductance per unit length L' and the capacitance per unit length C' of the wire is related to Z_C^0 via

$$Z_C^0 = \sqrt{L'/C'} = cL' = (cC')^{-1} \quad (A.2)$$

one has

$$L' \approx \frac{\mu_0}{2\pi} K_0(sr/c) \quad (A.3)$$

$$C' \approx 2\pi\epsilon_0/K_0(sr/c)$$

With these equations, the characteristic impedance for the lightning model of Figure 1c. can be formulated. Since for this model the currents flow mainly in the lightning channel of radius r_0 and the charges reside only on the effective corona surface of radius r_c , this lightning model will have a series impedance per unit length Z' and a shunt admittance per unit length Y' given by

END

FILMED

11-83

DTIC